Heliyon 8 (2022) e09600

Contents lists available at ScienceDirect

Heliyon

journal homepage: www.cell.com/heliyon

Research article

Synthesis, characterization, DFT analysis and docking studies of a novel Schiff base using 5-bromo salicylaldehyde and β-alanine

M.S. Meenukutty, Arsha P. Mohan, V.G. Vidya, V.G. Viju Kumar *

Department of Chemistry, University College, Thiruvananthapuram, Kerala, 695034, India

ARTICLE INFO

Keywords:
5-bromosalicylaldehyde
β-alanine
DFT
Molecular docking
PARP-Protein Swiss ADME

ABSTRACT

Poly(ADP-ribose) polymerase-1(PARP-1) is a DNA-dependent enzyme, forming part of ADP-ribosyltransferase family. Although some PARP inhibitors find therapeutical applications in cancer therapy and exhibits crucial role in DNA damage response. Here a novel Schiff base, (E)-3-((5-bromo-2-hydroxybenzylidene) amino) propanoic acid was synthesized using 5-bromo salicylaldehyde and β-alanine. Characterization was carried out using IR, UV-Vis, ^{1}H and ^{13}C NMR and mass spectrum. Present study involves the evaluation of a novel Schiff base as an inhibitor against human breast cancer cell lines (pdb:3GEY) using 2-(dimethylamino)-N-(6-oxo-5,6-dihydrophenanthridin-2-yl) acetamide (DDA) as a native ligand. In silico study of 3GEY inhibitor is a variant of PARP-15, docking with two different ligands (E)-3-((5-bromo-2-hydroxybenzylidene) amino) propanoic acid (SBL) and the native ligand. Synthesized ligandis docked in to the B chain of PARP enzyme binding site to visualize the best docked poseand favorable ligand-protein binding interactions. Swiss ADME tool determines the drug likeness and strongly suggests that SBL can be a promising candidate to fight against breast cancer. DFT studies were done to support the experimental results using B3LYP/6-311+G(d,p) and geometry optimization was performed. Various thermodynamic parameters and NLO properties were found out. ECD and VCD spectrum were explained using DFT studies. Vibrational and Raman frequencies were also reported. HOMO-LUMO band gaps, Mulliken charges were calculated and the electrostatic potential surface was mapped with various properties. Experimental findings obtained are in good agreement with that of theoretical DFT analysis.

1. Introduction

PARP inhibitor protein (Poly(ADP-ribose)polymerase) has DNA repairing properties so popularly called as guardian angel of DNA. It inhibits mitosis, inflammation, non prescription and cytotoxic properties [1]. Thus PARP-1 act as an anti-cancer agent while PARP inhibitors find applications as chemo-sensitizing agents in various kind of cancer growths [2, 3]. The parent PARP protein has six domains. Two of three in these six domains are Zn binding domains having the power to repair damaged DNA, and the third one is Zn binding domain that directs DNA-dependent enzyme activation [4, 5]. One of the domains of PARP-15 zinc finger is antiviral protein and it gives important antiviral response in mammals [6]. The isolated transferase domain of PARP-15 has considerable auto modification activity in *invitro* studies [7]. So pharmaceutical industries used PARP inhibitor protein as a new class of drug. Here amino acids in the active site of 3GEY is a variant of PARP target protein which makes interaction with a ligand containing functional groups. This protein has four ligands out of which one ligand is the active one. Higher score steric interaction between protein and ligand indicates its high binding affinity [1]. So, this ligand has a crucial part in DNA damage repair and enables to treat ovarian, fallopian tube, primary peritoneal and breast cancer [4]. Some recent studies were already reported with PARP protein and a novel Schiff base, 1,3,4-oxadiazoles, which was subjected to insilco analysis, against breast cancer cells. Molecular docking study by using Schrodinger software shows that enzyme shows a very high value of binding affinity against 1,3,4-oxadiazoles Schiff base [8].

5-bromosalicylaldehyde containing Schiff base have antitumor activity [9] is applied for manufacturing anti-cancer drug and Schiff bases has unique biological activity, can be used as low toxic in design and synthesis, and has got several applications like antibacterial and fungal, anti-inflammatory [10], anti-tubercular [11], anti-oxidant [12], and kills parasitic worms [13, 14]. A naturally occurring non-essential amino acid, β - alanine form part of carnosine, which in turn helps to buffer acid in muscles [15]may exhibit tumor progression [16], which has been most vastly investigated [17]. β-alanine treatment will bring out anti-tumor

* Corresponding author.
E-mail address: viju@universitycollege.ac.in (V.G. Viju Kumar).

https://doi.org/10.1016/j.heliyon.2022.e09600
Received 21 March 2022; Received in revised form 22 April 2022; Accepted 26 May 2022

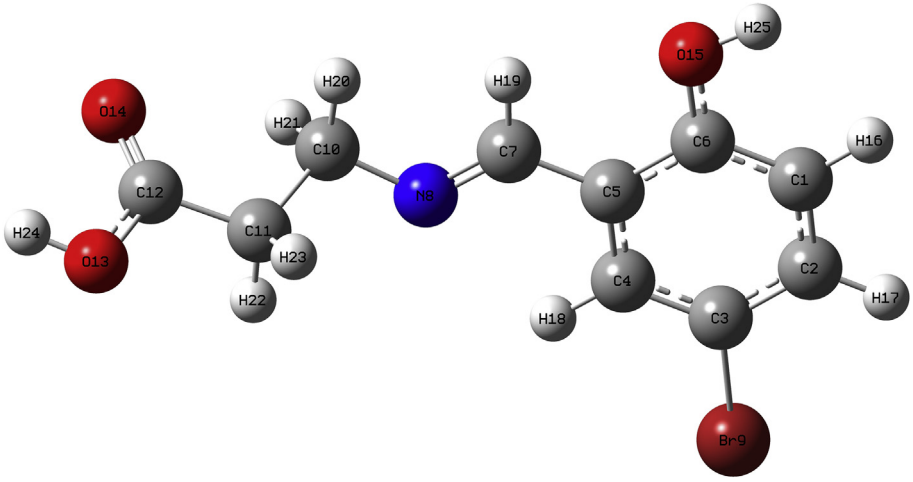

Figure 1. Optimized geometry of SBL.

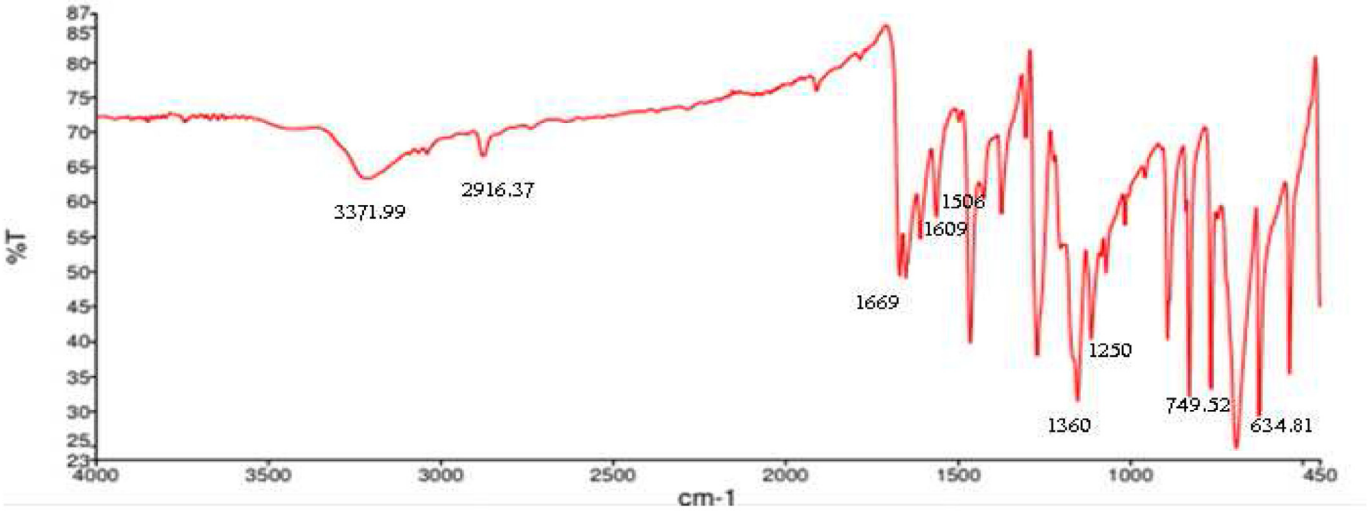

(a)Experimental

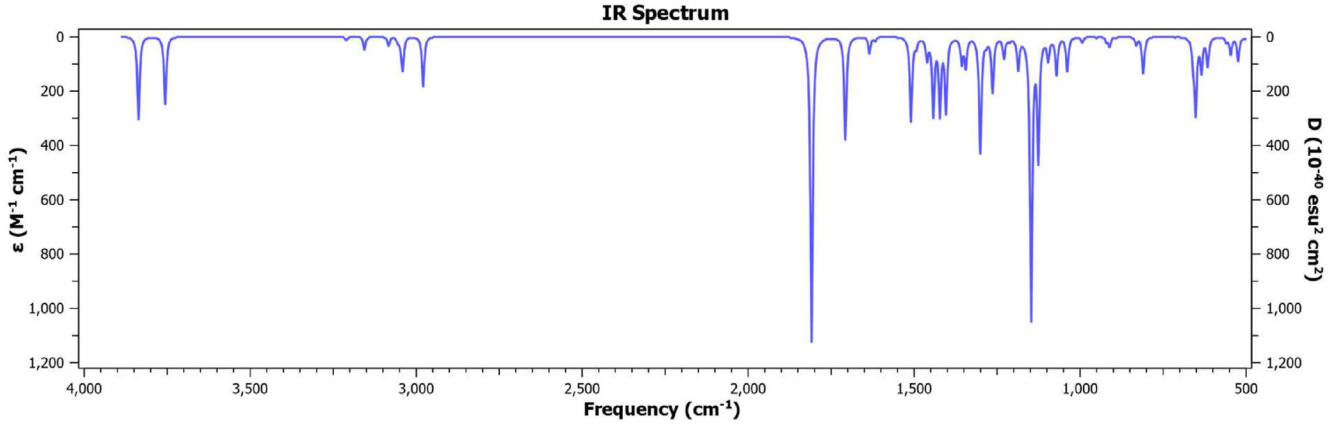

(b) Simulated

Figure 2. FT-IR spectra of SBL (a)Experimental (b) Simulated.

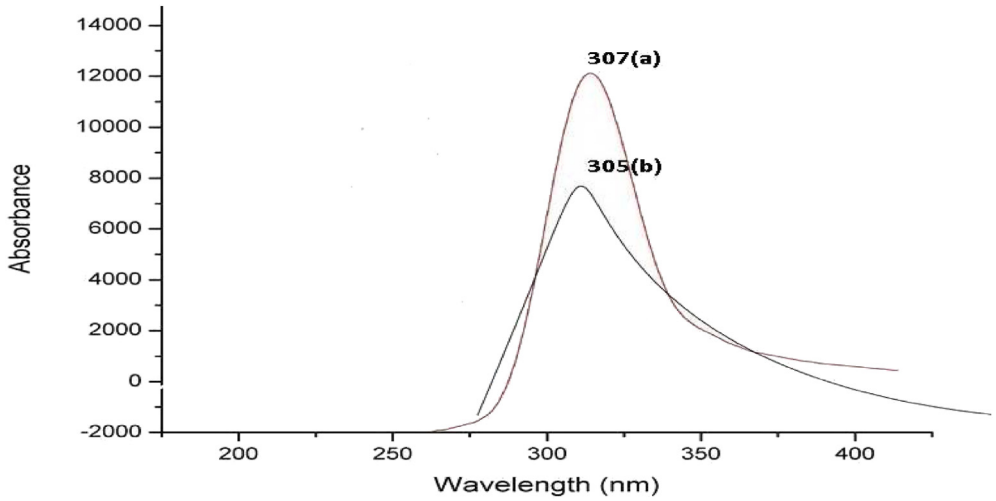

Figure 3. UV-Visible spectra of SBL (a) Experimental (b) Simulated.

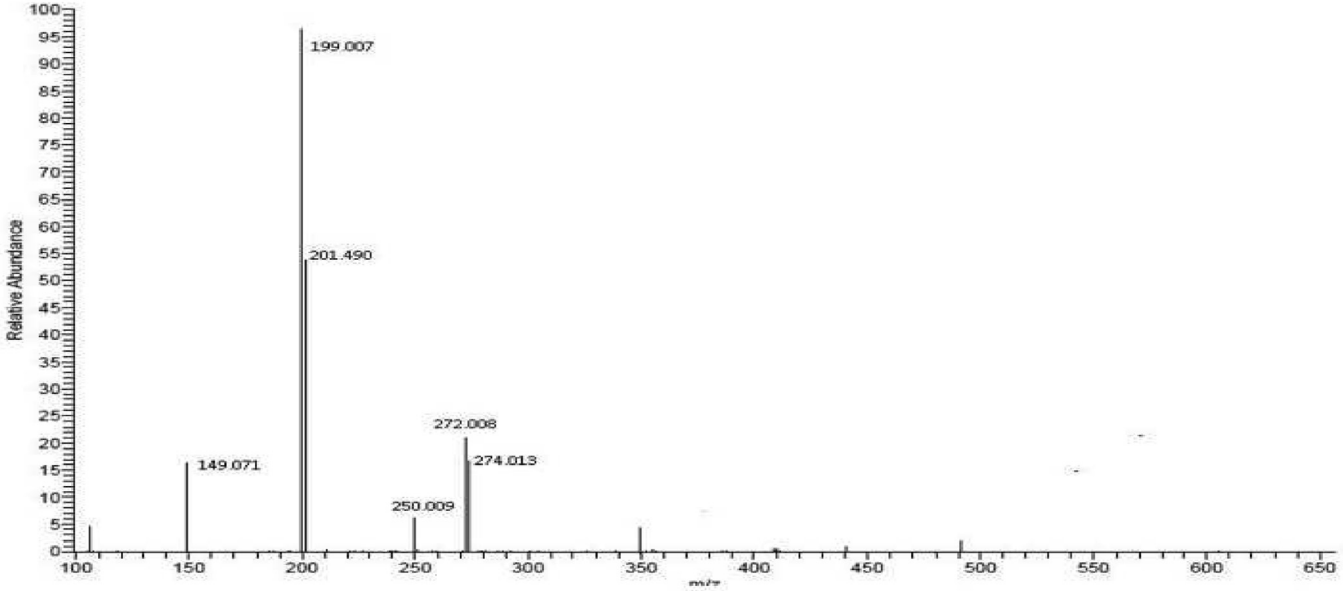

Figure 4. Mass spectra of SBL.

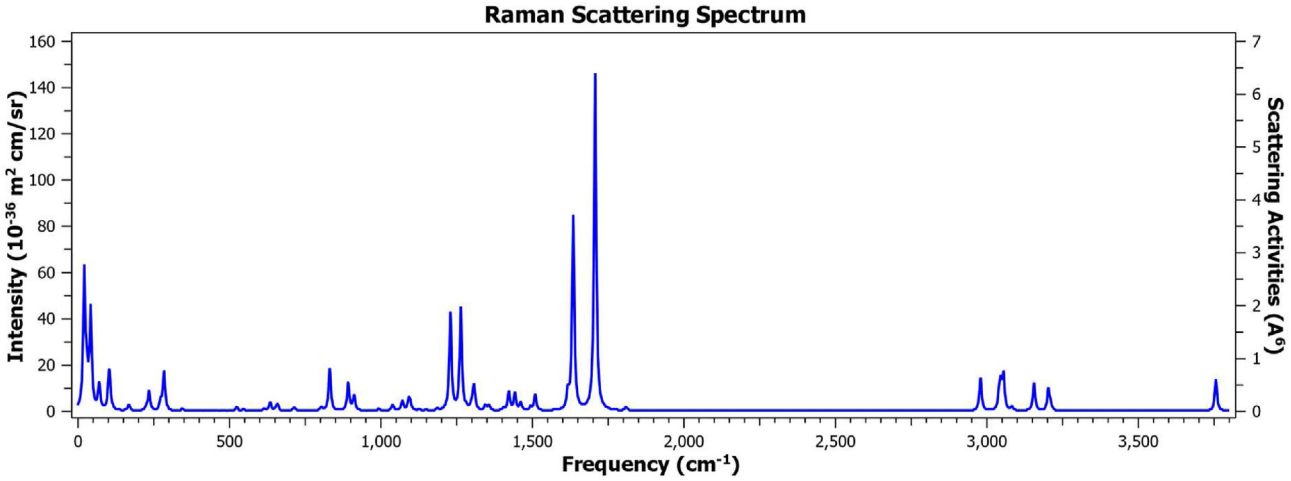

Figure 5. Raman spectra of SBL.

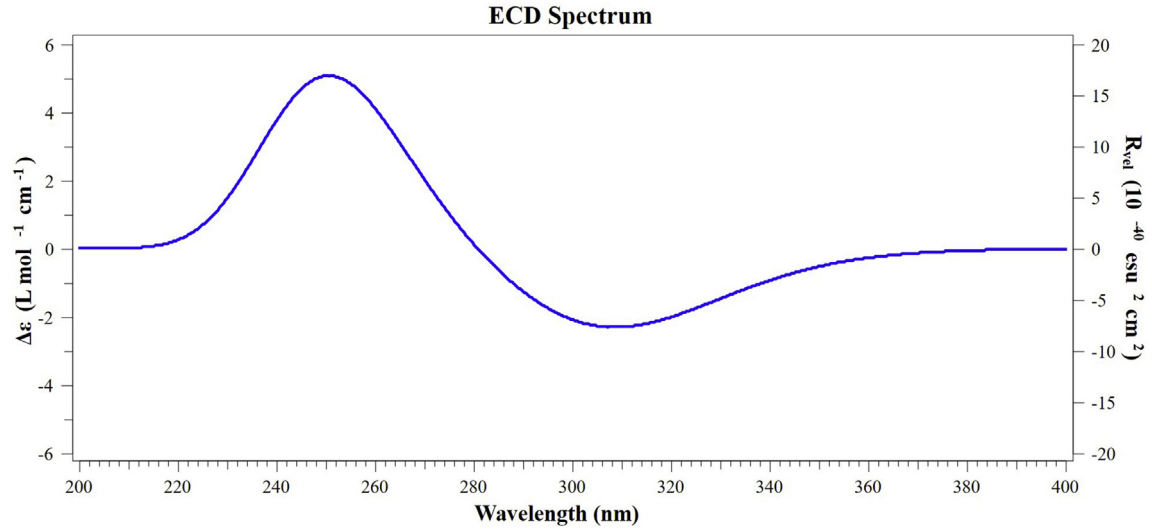

Figure 6. ECD spectrum of SBL.

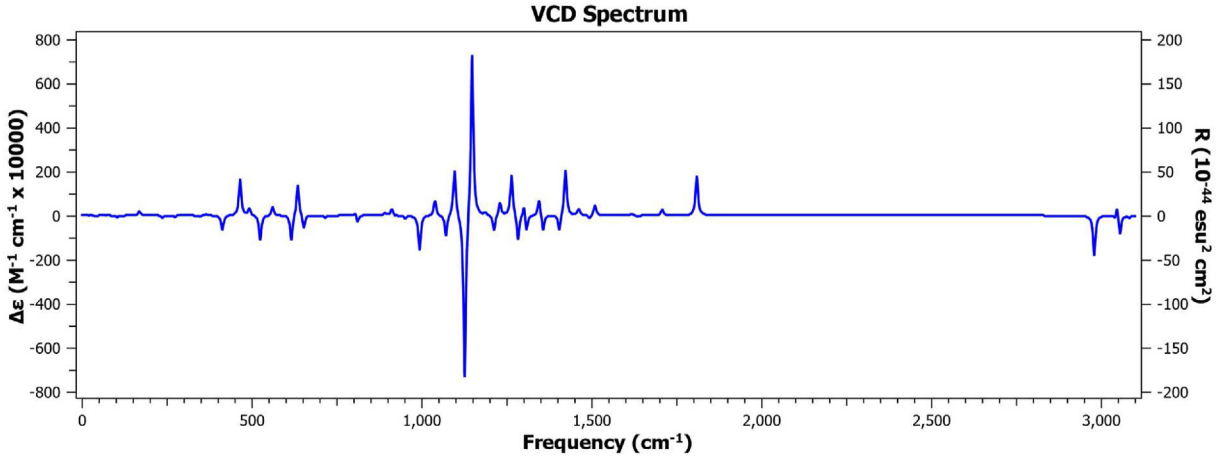

Figure 7. VCD spectrum of SBL.

results in selective tissues that express carnosine synthase [18]. When breast epithelial cells [19, 20] were treated with β-alanine, mechanism of action and specificity of the reagent need further investigation as a co-therapeutic agent in tumor treatment [21].

Schiff bases are much useful owing to their synthetic accessibility, structural features, and varieties. There have been many reported applications of antiviral activity and agriculture Schiff base has numerous applications in modern technology. It is used as photodetector in biological systems and used as a photo stabilizer and optical sound recording technology [12]. Schiff base ligands having oxygen and nitrogen donor atoms shows wide spectrum of biological properties. They can be used in homogeneous and heterogeneous catalysis [10]. Schiff bases possess an imine group –N=CH-, which is participating in transamination and racemization reactions [22]. Properties of Schiff base includeschelation [23], thermal stability [24], non-linear optical property [25], and proton transfer [26]. Thermally stable ones are used as stationary phases in gas chromatography [27]. The nonlinear optical property of Schiff bases provides applications in electronic, opto-electronic and photonic systems [28]. Schiff bases are used as catalysts in photo-electrochemical processes. They can also be used as corrosion inhibitors of mild steel, copper, aluminum, zinc etc. [27].

The present study focuses on the synthesis of novel Schiff base (E)-3-((5-bromo-2-hydroxybenzylidene) amino) propanoic acid (SBL) by the condensation reaction of 5-bromosalicylaldehyde & β alanine in a 1:1 ratio using ethanol as the solvent. The synthesized Schiff base Then Characterization was performed using IR, UV, ^{1}H and ^{13}C NMR and mass spectrum. Present work focus in silico study of 3GEY inhibitor is a variant of PARP-15, docking with two different ligands(E)-3-((5-bromo-2-hydroxybenzylidene) amino) propanoic acid (SBL) and2-(dimethylamino)-N-(6-oxo-5,6-dihydrophenanthridin-2-yl) acetamide (DDA). Here the SBL was optimized using DFT computational method [27]. Molecular docking into the protein 3GEY responsible for breast cancer, was carried out by evaluating binding affinities with SBL and finding drug-likeness using the SWISS ADME tool. Density functional theory calculations were done to support the experimental results using Gaussian16 W software. Visualization of results were done with GaussView 6.1software. B3LYP/6-311+G(d,p) level of theory was chosen for optimizing geometry of SBL. Various thermochemical parameters were reported. Vibrational and Raman frequencies was also reported. HOMO-LUMO band gaps, NLO Properties and Mulliken charge were calculated and the electrostatic potential surface was mapped with various properties [29].

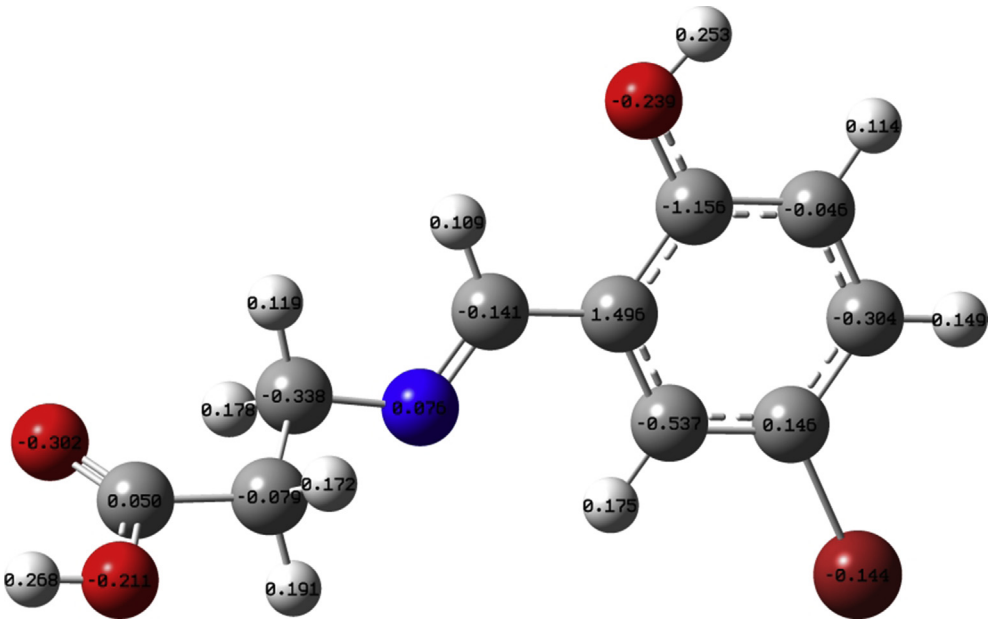

Figure 8. Mulliken charges.

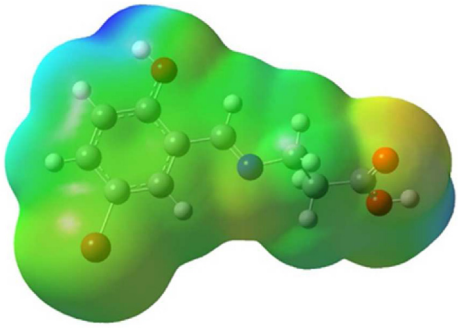

Figure 9. Plot of ESP on electron density surface.

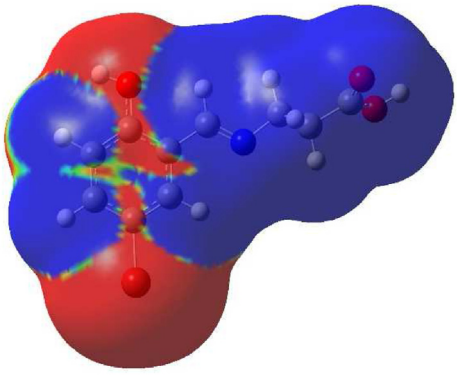

Figure 10. MEP plot of difference of SCF and Cl into ground state.

2. Experimental

2.1. Chemicals and instruments

All the chemicals used were of analytical grade and used without any further purification. 5-bromosalicylaldehyde, β-alanine and ethanol were purchased from Avra Chemicals. UV-Visible spectrumwas recorded in the range of 200–800 nm in PerkinElmer Lambda 365. IR spectrum of synthesized ligand in the frequency of 400-4000 cm^{-1} was recorded on Perkin Elmer spectrum IR version 10.6.1. ^{1}H and ^{13}C NMR spectrum was measured with 400 MHz Varian Joel spectrophotometer. HR-MS of the title compound was recorded using Accella 600 HPLC system with autosampler and PDA detector. DFT calculations were done using Gaussian 16W software and visualized using GaussView 6.1 software. Molecular docking was done using Auto Dock Vina v.1.2.0 tools.

2.2. Preparation

2.2.1. Synthesis of Schiff base

The Schiff base (E)-3-((5-bromo-2-hydroxybenzylidene) amino) propanoic acid [SBL] was synthesized by the condensation of 5-bromosalicylaldehyde and β-alanine [30] by dissolving each of the organic compounds separately in ethanolic solution in a beaker in 1:1 ratio. The solution in both the beakers are then poured onto RB flask which was then refluxed for about 4 h. A white colored compound formed was collected, filtered, recrystallized using ethanol, dried and characterized [29].

3. Results and discussions

3.1. Geometry optimization

The optimized geometry of synthesized ligand SBL (Figure 1) was done with B3LYP/6-311+G(d,p) level of accuracy. C_{10}–N_8 bond length is found to be 1.452A^0 and $C_7 = N_8$ bond length is about 1.271A^0. C10–N_8 bond length is slightly greater than $C_7 = N_8$, because double bonds have shorter bond distances than the single bond. C_6–O_{15} bond length is slightly less than C_{12}–O_{13}. The bond lengths of C_6–O_{15}, C_{12}–O_{13}, C_3–Br_9, $C_{12} = O_{14}$ and O_{15}–H_{25} are 1.368A^0, 1.357 A^0, 1.919A^0,1.205A^0 and 0.9628A^0 respectively. The bond length of benzene ring is given by C_1–C_2 is 1.39A^0, C_2–C_3 is 1.393A^0, C_3–C_4 is 1.384A^0, C4–C_5 is 1.402A^0, C_5–C_6 is 1.405A^0. C_4–H_{18} and C_2-H_{19} bond lengths are 1.081A^0 and 1.822A^0 respectively. The basic geometry of trigonal planar is 120^0. The bond angle of C_2–C_1–C_6 = 120.495^0, C_5–C_6–C_1 = 120.30^0, C_1–C_2–C_3 = 119.18^0, C_2–C_3–C_4 = 120.623^0, C_3–C_4–C_5 = 120.454^0, C_4–C_5–C_6 = 118.658^0. C_6–O_{15}–H_{25} bond angle is 109.94^0 whereas the C_{12}–O_{13}–H_{24} bond angle is 107.43^0. C_6–O_{15}–H_{25} angle is slightly greater than C_{12}-O_{13}-H_{24}, because the region with one double bond and single bond has got high electron density so that the double bond causes slightly larger angle

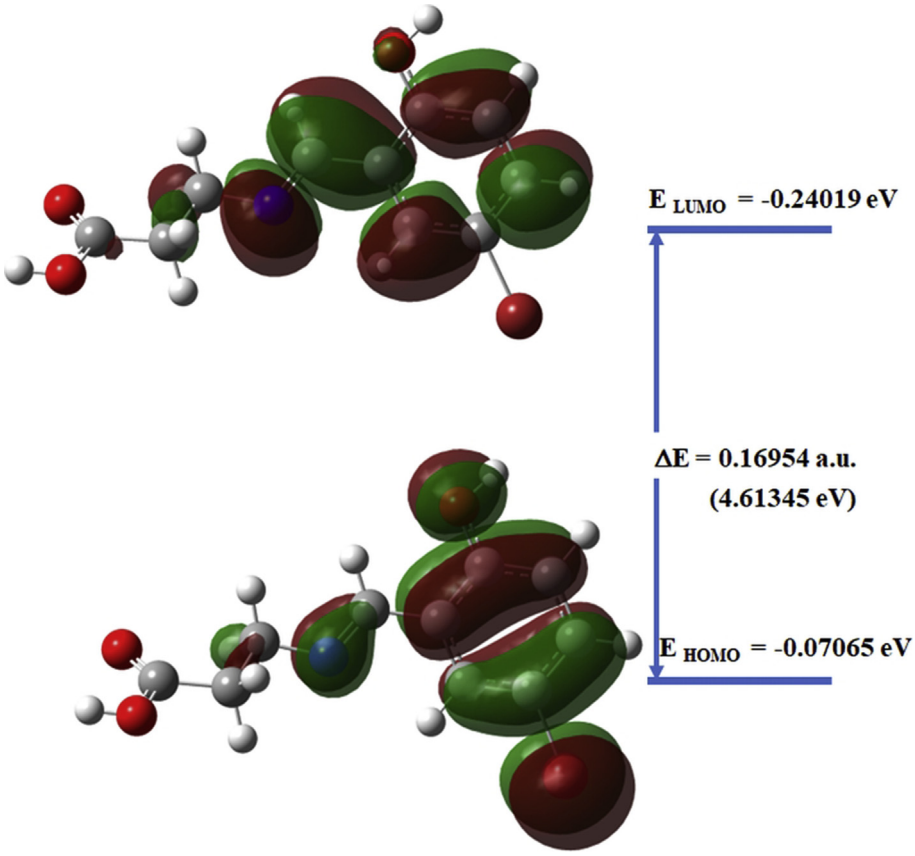

Figure 11. HOMO and LUMO of SBL

Table 1. Thermochemical data from DFT analysis.

Thermal energy	126.533 kcal/mol
Heat Capacity (CV)	53.567 Cal/mol-Kelvin
Entropy (S)	129.711 Cal/mol-Kelvin
Electronic Energy (EE)	-3241.852 Hartree
Zero-point Energy Correction	0.186738 Hartree
Thermal Correction to Energy	0.201643 Hartree
Thermal Correction to Enthalpy	0.202587 Hartree
Thermal Correction to Free Energy	0.140957Hartree

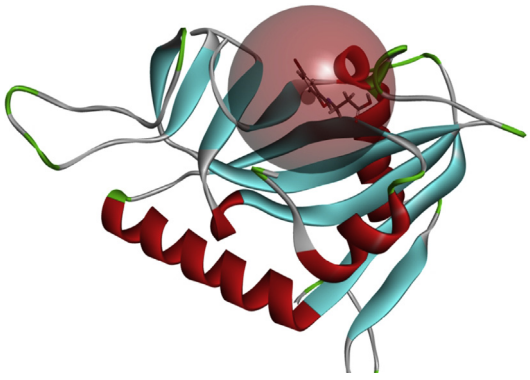

Figure 12. Ligand docked into the active site of B chain of 3GEY protein.

and angle between single bond is slightly smaller. They are attached with adjacent C=O bond, $H_{19}C_7N_8$ bond angle is 121.885^0 which is slightly greater than $H_{20}O_{10}N_8$ bond angle which is 112.57^0, $H_{22}–C_{11}–H_{23}$ is 105.821^0 and is slightly less than $H_{21}–C_{10}–H_{20}$ is 107.230 and $C_{11}–C_{10}–H_{21}$ is 108.169^0 which is greater than $C_{10}–C_{11}–H_{23}$ is 111.253^0. $O_{13}C_{12}O_{14}$ bond angle is about 122.345^0.

The dihedral angles are $H_{20}–C_{10}–N_8$ & $H_{19}–C_7–N_8–C_{10}$ which are-3.5539^0 and 0.5856^0 respectively.

3.2. FT- IR spectra

The IR spectra of the synthesized Schiff base SBL (Figure 2) exhibits strong absorption. The experimental value of $\nu_{C=O}$ appears at 1669 cm^{-1}. The intense band of $\nu C = N$ were observed at 1609 cm^{-1} [29]. ν_{C-H} stretching is observed at 2916.37 cm^{-1}. A sharp peak observed at 749.52 cm^{-1} corresponds to out π(C–H) interactions. A strong absorption observed at 1506cm^{-1}indicates benzene ring C=C backbone stretching vibration peak. Several peaks observed in the range of 2916-2429.3 cm^{-1} is due to the presence of aromatic C–H bond. The C–O stretching was observed at 1250-1360 cm^{-1} range with strong bands. The CH = N groups stretching vibrations appear at 2916.37 cm^{-1} and the band at 3371.99 cm^{-1} that does not include hydrogen bonding ν_{OH} [31]. The sharp peak obtained at 688.05 cm^{-1} is due to C–H bending. C–Br stretching is observed at 635.81 cm^{-1}.

Computed IR intensities of the novel compound SBL is calculated using B3LYP/6-311+G(d,p). A strong and broad peak of OH was obtained at 3208.76 cm^{-1}. The simulated result of SBL shows peak of $\nu C =$ O at 1650 cm^{-1}. The intense band of $\nu C = N$ were observed in the stretch at 1606 cm^{-1} νC–H stretching is observed at 2978 cm^{-1}. The sharp peak obtained at 713 cm^{-1} is C–H bending. The strong absorption at 1461-1442 cm^{-1} due to the presence of benzene ring C=C stretching vibrational absorption peak. C–O stretching appears at 1211-1300 cm^{-1}. The CH = N group stretching vibrations appear at 2978.90 cm^{-1}. The peak at 3082 cm^{-1} that not including hydrogen bonding can be assigned to νOH.

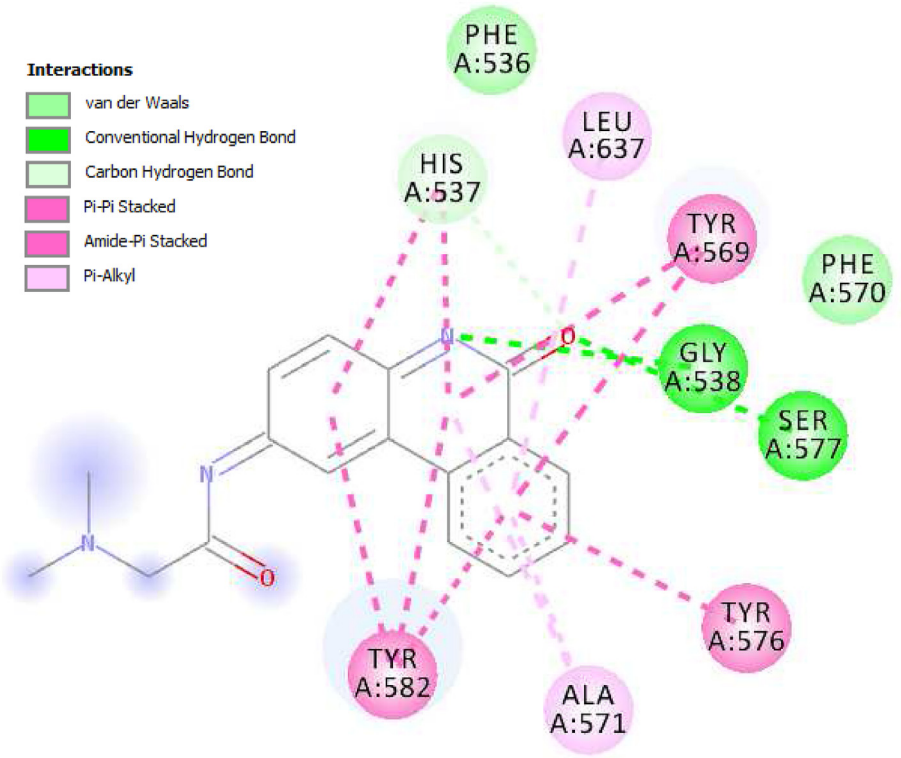

Figure 13. Binding interactions of native ligand.

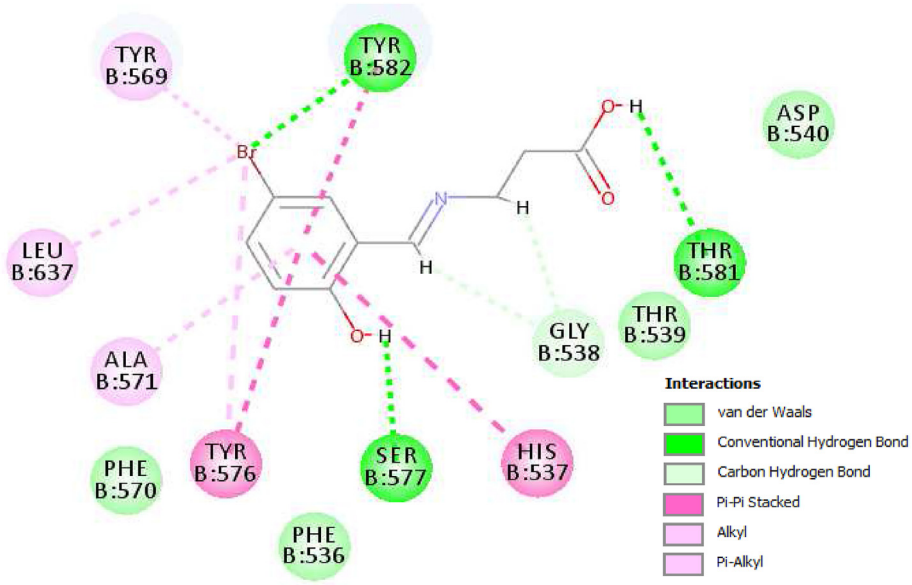

Figure 14. Binding interactions of synthesized ligand (SBL).

C–Br stretching is present at 634.39 cm^{-1}. A strong & broad peak of OH is obtained at 3210.81 cm^{-1} [32]. Experimentally observed FT-IR spectra of the title compound is in good agreement with that of the theoretical value.

3.3. UV-VIS spectra

The experimental and theoretical absorbance wavelength of the title compound SBL(Figure 3) were noted. The maximum absorbance wavelength of SBL was measured to be 307 nm experimentally. UV-Vis spectra were computed with TD-DFT. The theoretical maximum absorption wavelength is 305 nm which indicates the excitation of electrons of azomethine group [33]. This is attributed to the azomethine group's π-*π and n-*π transitions [34]. Thus, experimentally determined absorption wavelength of SBL agrees well with that of the theoretical value.

3.4. High resolution mass spectra

The mass spectral fragmentation of the synthesized Schiff base SBL (Figure 4) can be studied using mass spectrometry. SBL was characterized using HR-MS spectra. Since one Bromine atom present in the synthesized compound causes two peaks in the molecular ion region i.e.; M+ and

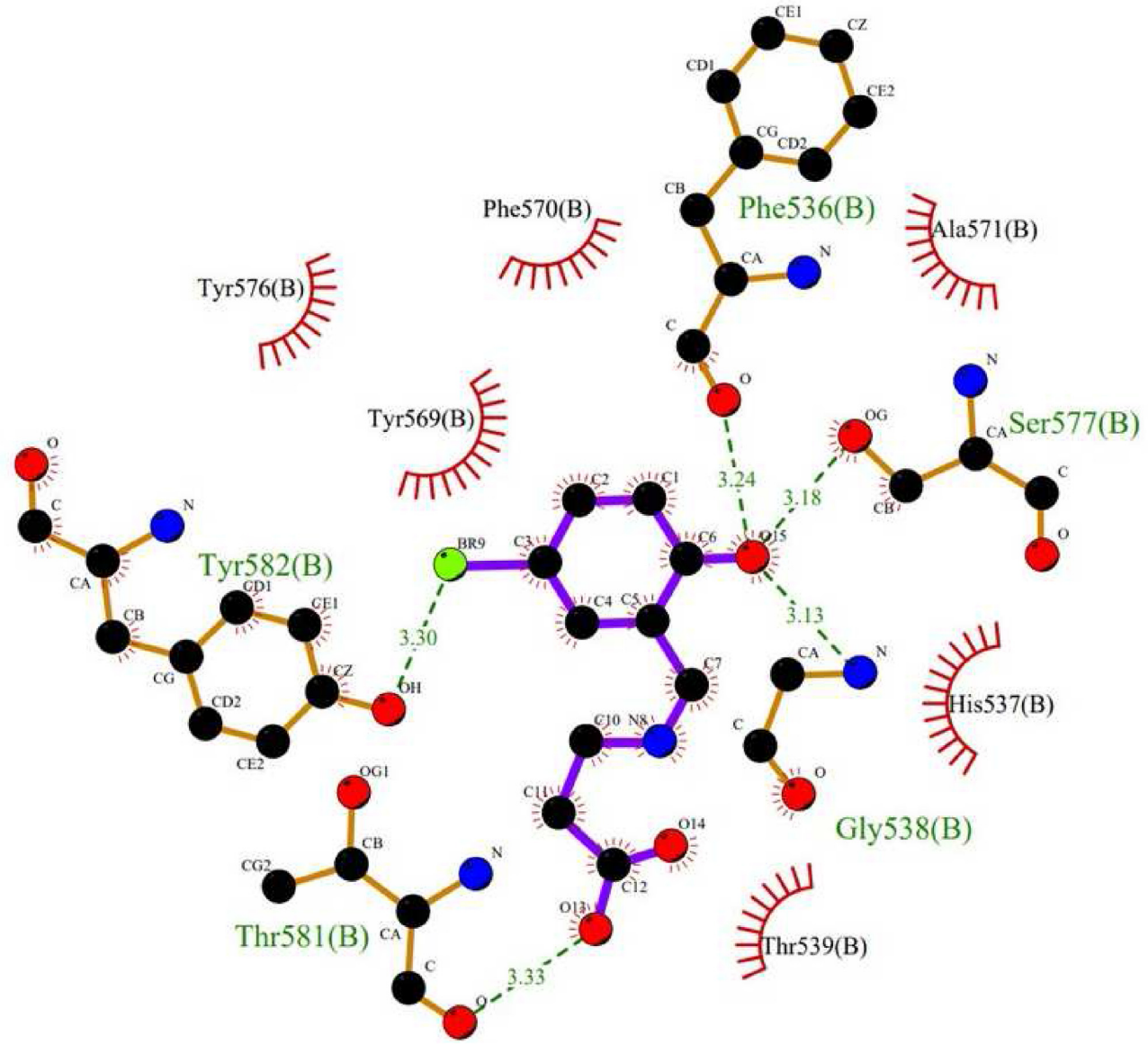

Figure 15. Protein ligand (SBL) interaction in LigPlot.

M+2. $M^+ = 272.008$ and M+2 = 274.013. The molecular weight of the synthesized compound C10H10O3NBr is 272.008 g/mol and the base peak is at m/z = 199.007($C_7H_5OBrN^+$).

3.5. Raman spectra

The synthesized Schiff base SBL (Figure 5) waschecked for Raman vibrations calculated using B3LYP/6-311+G (dip) functional. Bands at 1634 cm^{-1} and 1707cm^{-1}corresponds to C=N&C=O stretching frequencies respectively. Bands at 3082,3054,3045, cm^{-1} correspond to C–H stretching modes of the phenyl ring and the sharp peak obtained at 713 cm^{-1} corresponds to out of plane π(C–H) interactions. Then a strong absorption at 1493-1403 cm^{-1} is due to the presence of benzene ring C=C stretching band. C–O stretching frequency were shown by bands in the region 1211-1038 cm^{-1}. C–Br stretching frequency band is found at 634 cm^{-1}. C–OH Stretching frequency is shown by bands in the region 1211-1038 cm^{-1}.

3.6. ^{13}C & ^{1}H NMR spectra

For the title compound, the experimental ^{1}H and ^{13}C NMR was measured using a 400 MHz Varian Joel instrument using $CDCl_3$ as the solvent. Experimentally measured ^{1}H NMR spectra of SBLshowed two sharp singlets which were interpreted for OH δ at 10.918 (s,1H,OH) due to the carboxylic part of OH and δ 11.61 (s,1H, OH) which is due to the aromatic OH proton [23]. ^{1}H NMR (δ, ppm, $CDCl_3$, 400 MHz) 7.66 (s, 1H, CH), 7.605 (s, 1H, CH), 7.43 (s, 1H, CH), 3.6 (t, 2H, CH_2), 2.73 (t, 2H, CH_2). The sharp singlet in 7.66 ppm attributed to azomethine(-HC = N-) proton.^{13}C NMR (δ, ppm, $CDCl_3$, 400 MHz) δ 119.46 (C_1), 129.90 (C_2), 137.8 (C_3), 135.7(C_4), 139.8 (C_5), 160.6 (C_6), 155.5 (C_9), 66 (C_{11}), 38 (C_{12}), 174 (C_{13}). The signals near δ160.6 (C_6)-174(C_{13}) ppm due to azomethine carbon atoms [35]. Theoretically, ^{1}H NMR values were δ 11.09 (s, 1H, OH), 9.79 (s, 1H, OH), 7.58 (s, 1H, CH), 7.600 (s, 1H, CH), 8.41 (s, 1H, CH), 3.30 (t, 2H, CH_2), 2.66 (t, 2H, CH_2); ^{13}C NMR values were δ 118 (C_1), 129(C_2), 138.9 (C_3), 136.7 (C_4), 139.4 (C_5), 161.9 (C_6), 158.5 (C_9), 62.2 (C_{11}), 36.4 (C_{12}), 177 (C_{13}). Thus, both experimentally measured ^{1}H and ^{13}C NMR spectra results are in good agreement with that of theoretical values.

3.7. ECD and VCD spectrum

The differential absorption of left and right circularly polarized light linked with the electronic transitions of chromophores present in a

Table: 2. Swiss ADME tool data of two ligands.

Properties	$C_{10}H_{10}BrNO_3$(SBL)	$C_{17}H_{17}N_3O_2$(native ligand)	A drug like property exhibiting a range
Physicochemical			
1.Molar refractivity	61.01	88.90	40–130
2.TPSA	69.89 A^0	65.20A^0	20–130
Lipophilicity			
1.iLOGP	1.68	2.01	
2.xLOGP3	1.33	1.71	
3.wLOGP	2.05	1.99	Lipophilic compound
4.Mlogp	1.44	1.92	Value < 5
5.SILICO8-IT	2.48	2.69	
Water solubility			
1.LOGS	-2.40	-2.69	<-10 is soluble
2.solubility	1.09 mg/ml	5.96 mg/ml	
Pharmacokinetics			More -ve value high skin permeability
1. Log k_p	-7.02	-6.89	
Drug likeness			
1.Bioavailabilityscore	0.85	0.55	Amount of dose get human body
Medicinal chemistry 1.synthetic accessibility	2.30	2.12	<5 Easy synthesis >5 hard to synthesis Range 1-10

molecule is referred to as Electronic Circular Dichroism (ECD). The ECD spectrum of the title compound is found near UV region 309.20 nm(Figure 6), indicating the existence of an aromatic chromophore in the compound, according to DFT analysis the absorbance reported by their UV-Vis spectra at 307 nm is similar to this peak of absorption at 309.20 in the ECD spectrum.

ECD is extended from the UV to the IR area of the electromagnetic spectrum by vibrational circular dichroism (VCD) (Figure 7). The C=N stretching vibration is represented by a peak at 1616 cm^{-1} in the estimated VCD spectra. The absorption peak of vC = O in VCD bands is 1669 cm^{-1}. The presence of a benzene ring C=C backbone stretching vibration absorption peak could explain the significant absorption at 1678 cm^{-1}. At 3046 cm^{-1}, the VCD spectrum displays a substantial C–H stretching. All of these estimated VCD spectra results are in good agreement with the IR spectral results.

3.8. Mulliken charge

Mulliken charges are obtained from Mulliken population analysis and estimates partial atomic charges, based on the linear combination of atomic orbitals and molecular orbital techniques. The For the title compound (Figure 8) C_5 atom occupies the higher positive value 1.495515 and becomes more acidic. For the molecule C_1, N_8, C_{12}, H_{19} and H_{20} atoms occupies the low positive values such as 0.046061, 0.076062, 0.049685, 0.109121 and 0.119319 respectively and becomes less acidic as compared to other higher positive values. Here nucleophilic attack is preferred over electrophilic attack. The one Br atom present have a negative value of -0.144061. An increased electron density (negative charge) can be found at C_7, C_{10}, C_{11}, O_{13}, O_{14} and O_{15} with values -0.141115, -0.337749, -0.078615, -0.210919, -0.301892 and -0.239074 respectively. It is found out that the electrophilic substitution is more preferred at these positions rather than nucleophilic substitution.

3.9. Non -linear optical properties (NLO)

NLO properties are derived from the interaction of electromagnetic fields and electrons in the molecule which results in altered frequency, phase, amplitude and propagation features, resulting in non-linear visual phenomena [29]. In the DFT level, the electronic dipole moment, molecule polarizability, first and second-order hyper-polarizability values can be calculated to evaluate NLO property. The polarizability, hyperpolarizability, and dipole moment of the title chemical were determined using Gaussian program, with polarizability being 166.131au. The dipole moment was found to be 3.580 Debye, and these findings clearly show that the examined molecule has nonlinear optical behavior [36].

3.10. Molecular electrostatic potential (MEP)

The MEP surface picturizes the reactiveness against positive or negative reactants and attributes structure-activity relation of the system [37]. There exists a correlation between electrostatic potential and the dipole moment, electronegativity, and partial charges [38]. Near the phenyl ring, the greatest positive region is located, and zero potential spans over the remaining moieties. The strongest attraction is indicated by blue region, and the strongest repulsion is in red region. The blue colored positive regions are susceptible to nucleophilic reactivity and red negative regions were attributed to electrophilic reactivity. Negative potential is attributed to the presence of lone pairs in the electronegative atoms. In SBL, the negative region is localized over C=N and positive region near the phenyl group. The remaining surface isencapsulated by zero potential as shown in Figure 9. The difference in electron density between the first excited state from the total CI density matrix from TD-DFT calculation and ground state electron density from total SCF density is mapped onto the SCF density shown in Figure 10. The Blue region indicates positive values of difference in electron density where the ground state density is smaller than the excited state density. The red region indicates the reverse. Here in the present system electron density moves from phenyl moiety to C=N moiety as transition happens from the ground state to first excited state.

3.11. Frontier molecular orbital analysis (FMO)

The energy values of the HOMO and LUMO orbitals are very important in quantum chemistry with the HOMO being the valence orbital that give out electrons, whilst the LUMO accepts electrons [39].

The electron in HOMO is more concentrated in the aromatic side and C=N bond, whereas in LUMO (Figure 11), the electron moves towards the aromatic side with Br atom and OH group the HOMO electron move away from the aromatic to aliphatic side, The energy gap is the difference in energy between the HOMO and LUMO orbitals, and it is an essential structure stability reflector [40]. In terms of charge transfer in compounds, a smaller HOMO-LUMO gap suggests that the molecule is less stable [41]. The conjugated molecules have a small HOMO-LUMO gap, which is due to a high degree of intramolecular charge transfer from the electron donor to the acceptor groups [30, 42]. The HOMO and LUMO energy values, in this case, are -0.24019 and -0.07065eV, respectively. I = E_{HOMO} = -0.24019 eV can be used to express the ionization energy and electron affinity. The hardness and chemical potential are calculated using the equations (I- A)/2 and (I + A)/2, where I and A are the chemical species' initial ionization potential and electron affinity, respectively [43]. The HOMO-LUMO energy gap is 4.613454664 eV for the title compound, with Ionization potential I = E_{HOMO} = -0.24019 eV, Electron affinity A = E_{LUMO} = -0.07065 eV, Global hardness = -0.5 eV, and Chemical potential = -0.08477 eV [44].

3.12. Thermochemistry

Thermodynamic property of the synthesized Schiff base (E)-3-((5-bromo hydroxy benzylidene) amino) propanoic acid obtained through DFT calculations are shown in Table 1.

4. Molecular docking

Synthesized Schiff base SBL were carried out for the molecular docking to measure the inhibition tendency of the target cancer protein 3GEY (Figure 12) which is the variant of PARP-15 [45]. Auto Dock vina v.1.2.0 was employed for molecular docking studies. For in silico screening, molecular docking is a functional tool in the arsenal of drug design experiments [46, 47]. Docking is a computer approach for finding a molecule that fits the protein's biologically active binding site energetically and geometrically [48, 49]. Molecular docking has proven to be an effective approach for discovering new drugs that target proteins. Protein-ligand docking refers to search for the most error-free and stable ligand conformation or pose with a protein on a specific binding site [50, 51]. For molecular docking, the target protein PDB file 3GEYis obtained from RCSB-Protein data bank and SBL ligand was saved in PDB format from Gaussian 16W. The simulation of protein-ligand binding interactions is done through Autodock tools (v. 1.5.6) and Auto Dock Vina. For preparing protein, water molecules were removed followed by adding polar hydrogens and Kollman charges. Auto grid determines the position of native ligand on binding site on B chain of target protein by arranging grid coordinates. In docking process, the coordinates of the grid box shall be validated for ensuring for the ligands to bind on binding site in the accurate conformation. Using Auto Dock Vina biologically active conformations are simulated and lower energy scores demonstrate the best protein-ligand binding affinity. Visualization of docked poses of SBL with the protein target was done using BIOVIA Discovery Studio visualizer 2021 (64 bit) client.

Figures 13 and 14 visualizes 2D interaction diagram of the best pose for the native ligand of protein and SBL respectively. Figure 14 provides protein-ligand (SBL) interaction in LigPlot. LigPlot V.4.5.3 is a tool which createsgraphicalrepresentation of protein-ligand interaction obtained from the three-dimensional coordinates incorporated in a pdb file of docked system (Figure 15). The interaction involves H-bonds designated as dashed lines and hydrophobic interactions indicated by Arc with Spokes directing towards contracting ligand atoms [52]. A total of ten amino acids are involved in ligand binding pocket of receptor for the native ligand with prominent interactions while 13 amino acids contribute to SBL ligand binding process.

The affinity of SBL ligands with receptor PARP-15 (pdb:3GEY) is given by prominent interactions to TYR 582, TYR 569, LEU 637, SER 577, GLY 538, THR 581, ALA 571 and these are the active residues in 3GEY target protein. Native ligand $C_{17}H_{17}N_3O_3$ illustrate HIS 537, LEU 637, TYR 569, GLY 538, TYR 576, TYR 582, ALA 571 and which indicate two different ligands have mostly similar active residues. There are two key residues that have hydrogen bonds SER577, GLY 538 which restricted ligand in the binding domain. C=N bond interacts with an amino acid residue (GLY 538) in both cases. Compare to native ligand, SBL has extra three residual interactions with bromine atom they are TYR 569, LEU 637, TYR 582. Here the native ligand is replaced with SBL is the easy process they docked in to the active site of 3GEY protein by key and lock method. So, at this time we can conclude that biological features of native ligand are similar to SBL, SBL being lower molecular weight system compare to native ligand and therefore, easy to trap in to the cavity.

The comparison chart reveals that some properties are favorable to SBL or comparable to that of native ligand which means SBL have potential drug likeness (Table 2). Here lipophilicity values are very much less than 5 in case of SBL which shows high Lyophilic character. Based on pharmacokinetics, more negative is the value has high skin permeability. Here SBL has got higher negative value of -7.02 where native ligand has got a value of -6.89 which mean that synthesized Schiff base shows high permeability through skin. The molecular weight of SBL is lesser than the native ligand and method of synthesis lot more easily than native ligand. From all these comparisons we can conclude that the SBL is way much better than the native ligand.

5. Conclusion

Bioinorganic chemistry is a prosperous field of drug research for cancer treatment so this Schiff base can be studied *invitro* study against PARP. Breast cancer is the most frequently detected cancer which accounts for 23% of the cancer cases and 14% of the cancer deaths. Over the past few years, Schiff bases find applications in medicine having multi-dimensional properties. Present study involves the synthesis of a Schiff base (E)- 3-((5-bromo-2-hydroxybenzylidene) amino) propanoic acid using 5-bromosalicylaldehyde and β-alanine. FT-IR, UV-Visible, ^{1}H &^{13}C NMR and mass spectrum studies were used to characterize the synthesized compound. FT-IR spectrum indicates a strong band in 1609 cm^{-1} which indicates $\nu_{C=N}$ bond. The maximum absorption in the UV-Vis spectrum is found at 307 nm. A molecular ion at $m/z = 274$ was observed in the mass spectrum, which matches to the molecular weight of the synthesized Schiff base with the molecular formula $C_{10}H_{10}O_3NBr$. The formation of the proposed compound was supported by ^{1}H and ^{13}C NMR. The experimental values are found to be in good agreement with theoretical values derived from DFT analysis. DFT analysis were carried with B3LYP/6-31+G(d, p), and the optimized geometry of the system was reported. Mulliken atomic charges and HOMO-LUMO band gaps were also determined. In this study, we aim to investigate how 3GEY, the variant of PARP-1 protein has high potent binding affinities between native ligand and SBL and comparison of interaction between ligand functional group with amino acid residues in protein employing Auto Dock tools. Visualization of docked pose of new Schiff base ligand shows promising interactions with active site residues of target protein. The drug likeness properties reported by using Swiss ADME tool also point towards a promising inhibitor candidate. The synthesized Schiff base, SBL can be further extended for its complex formation with different transition metal ions for enhanced biological activity.

Declarations

Author contribution statement

Meenukutty M. S, Arsha P Mohan: Performed the experiments; Analyzed and interpreted the data; Contributed reagents, materials, analysis tools or data; Wrote the paper.

Vidya V. G, Viju Kumar V. G: Conceived and designed the experiments; Analyzed and interpreted the data; Contributed reagents, materials, analysis tools or data; Wrote the paper.

Funding statement

This research did not receive any specific grant from funding agencies in the public, commercial, or not-for-profit sectors.

Data availability statement

Data will be made available on request.

Declaration of interests statement

The authors declare no conflict of interest.

Additional information

No additional information is available for this paper.

References

[1] F.J. Bock, P. Chang, New directions in poly(ADP-ribose) polymerase biology, FEBS J. 283 (2016).
[2] C.R. Calabrese, R. Almassy, S. Barton, M.A. Batey, A.H. Calvert, S. Canan-Koch, Anticancer chemo sensitization and radio sensitization by the novel poly(ADP-ribose) polymerase-1 inhibitor AG14361, J. Natl. Cancer Inst. 96 (2004).
[3] R. Plummer, C. Jones, M. Middleton, R. Wilson, J. Evans, A. Olsen, et al., Phase I study of the poly (ADP-ribose) polymerase inhibitor, AG014699, in combination with temozolomide in patients with advanced solid tumors, Clin.Cancer 14 (2008).
[4] M. Altmeyer, S. Messner, P.O. Hassa, M. Fey, M.O. Hottiger, Molecular mechanism of poly(ADP-ribosyl)ation by PARP1 and identification of lysine residues as ADP-ribose acceptorsites, Nucleic Acids Res. 37 (2009).
[5] Z.H. Tao, P. Gao, H.-W. Liu, Identification of the ADP-ribosylation sites in the PARP-1 auto modification domain: analysis and implications, J. Am. Chem. Soc. 131 (2009).
[6] M.-F. Langelier, K.M. Servent, E.E. Rogers, J.M. Pascal, A third zinc-binding domain of human poly(ADP-ribose)polymerase-1 coordinates DNA-dependent enzyme activation, J. Biol. Chem. 283 (2008).
[7] J.E. Tyczynski, I. Plesko, T. Aareleid, M. Primic-Zakelj, M. Dalmas, J. Kurtinaitis, A. Stengrevics, D.M. Parkin, Breast cancer mortality patterns and time trends in 10 new EU member states: mortality declining in young women, but still increasing in the elderly, Int. J. Cancer 112 (2004).
[8] M.F. Langelier, D.D. Ruhl, J.L. Planck, W.L. Kraus, J.M. Pascal, The Zn3 domain of human poly(ADP-ribose) polymerase-1 (PARP-1) functions in both DNA-dependent poly(ADP-ribose) synthesis activity and chromatin compaction, Biol. Chem. 285 (2010).
[9] Narayan Shridhar Deshpande, Gowdru Srinivasa Mahendra, Natasha Naval Aggarwal, Banylla Felicity Dkhar Gatphoh, Bistuvalli Chandrashekharappa Revanasiddappa, Insilico design, ADMET screening, MM-GBS binding free energy of novel 1,3,4 oxadiazoleslinked Schiff bases as PARP-1 inhibitorstargeting breast cancer, Fut. J. Pharmaceut. Sci. 7 (2021).
[10] C. Renner, A. Asperger, A. Seyffarth, J. Meixensberger, R. Gebhardt, F. Gaunitz, Carnosine inhibits ATP production in cells from malignant glioma, Neurol. Res. 32 (2010).
[11] B.S. Sathe, E. Jayachandran, V.A. Jagtap, G.M. Sreenivasa, Synthesis and antibacterial, antifungal activity of novel analogs of fluoro benzothiazole Schiff bases, J. Chem. Pharmaceut. Sci. 3 (2010).
[12] T. Aboul-Fadl, F.A.-H. Mohammed, E.A.-S. Hassan, Synthesis, antitubercular activity and pharmacokinetic studies of some schiff bases derived from 1-alkylisatin and isonicotinic acid hydrazide (inh), Arch Pharm. Res. (Seoul) 3 (2003).
[13] D. Wei, N. Li, G. Lu, K. Yao, Synthesis, catalytic and biological activity of novel dinuclear copper complex with Schiff base, Sci. China, Ser. B 49 (2006).
[14] P.G. Avaji, C.H. Vinod Kumar, S.A. Patil, K.N. Shivananda, C. Nagaraju, Synthesis, spectral characterization, in-vitro microbiological evaluation and cytotoxic activities of novel macrocyclic bis hydrazone, Eur. J. Med. Chem. 44 (2009).
[15] Ei 1obasuyi, O. 2iyekowa, Synthesis, Characterization and antimicrobial of schiff base from 5-bromo –salicylaldehyde and P-toluidine, J. Appl. Sci. Environ. Manag. 22 (2018).
[16] F. Gaunitz, A.R. Hipkiss, Carnosine and cancer: a perspective. Amino Acids, J. Cheminform. 43 (2012).
[17] Crystal Y. Wilson, Sathiyanarayanan Velayudham, Sundar Manickam, Easwaramoorthy Deivanayagam, β - tolyl alanine derived schiff base complexes –synthesis characterization and antimicrobial assessment, J. Pharmaceut. Sci. Res. 7 (2015).
[18] R.C. Harris, M.J. Tallon, M. Dunnett, L. Boobis, J. Coakley, H.J. Kim, J.L. Fallowfield, C.A. Hill, C. Sale, J.A. Wise, The absorption of orally supplied beta-alanine and its effect on muscle carnosine synthesis in human vastus lateralis. Amino Acids, BMC Mol. Cell Biol. 30 (2006).
[19] S.M. Sondhi, N. Singh, A. Kumar, O. Lozach, L. Meijer, Synthesis, anti-inflammatory, analgesic and kinase (CDK-1, CDK-5 and GSK-3) inhibition activity evaluation of benzimidazole/benzoxazole derivatives and some schiff's bases, Bioorg. Med. Chem. 14 (2006).
[20] B. Preethi1, R. Jayaprakash2, S. Kutti Rani1*, N. Vijayakumar, Characterization, molecular docking, antimicrobial and anticancer studies on 5-Bromosalicylalde-hyde-furan-2-yl-methanamine condensed schiff base rare earth metal complexes, Asian J. Chem. 1252 (2021).
[21] BalakrishnaGowdhami SubramanianAmbika, Balakrishnan Karthiyayini, Venkatesan Ramya, Balamuthu Kadalmani, R.T.V. Vimala, Mohammad A. Akbarsha, Potential application of two cobalt (III) Schiff base complexes in cancer chemotherapy: leads from a study using breast and lung cancer cell, Nat. Cent. Biotechnol. Inform. 75 (2021).
[22] C. Ajit Kumar, S.N. Pandeya, Synthesis and anticonvulsant activity (chemoshock) of schiff and mannich bases of isatin derivatives with 2-amino pyridine (mechanism of action), Int. J. PharmTech Res. (2012).
[23] P. Hohenberg, W. Kohn, Inhomogeneous electron gas, Phys. Rev. 136 (1964).
[24] H. Schiff, Mittheilungen aus dem Universitätslaboratorium in Pisa: eine neue Reihe organischer Basen, Annal. der Chem. Pharm. 131 (1864).
[25] Hamed Soleymanabadi, Somayeh F. Rastegar, Theoretical investigation on the selective detection of SO2 molecule by AlN nanosheets, J. Mol. Model. 20 (2014), 2014-01-01.
[26] Hamed Soleymanabadi, Somayeh F. Rastegar, DFT studies of acrolein molecule adsorption on pristine and Al-doped graphenes, J. Mol. Model. 19 (2013).
[27] D. Music, R.W. Geyer, J.M. Schneider, Recent progress and new directions in density functional theorybased design of hard coatings, Surf. Coating. Technol. 286 (2016).
[28] S.G. Kaplan, L.M. Hanssen, Standard Reference materials.Infrared Transmittance Standard – SRMS 2053,2054,2055 and 2056, NIST Special Publication, 2001.
[29] Jang Bahadur Khadka1, Bhawani Datt Joshi2, Molecular electrostatic potential, HOMO-LUMO and vibrational study of aristolochic acid II using density functional theory, Bibechana 12 (2014).
[30] R.B. Moffett, N. Rabjohn, Organic syntheses, Division of organic synthesis, J. A-Z (2018).
[31] Khlood S. Abou Melha, Gamil A. Al-Hazmi, Althagafi Ismail, Arwa Alharbi, Ali A. Keshk, Fathy Shaaban, Nashwa El-Metwaly, Spectral, molecular modeling, and biological activity studies on new schiff's base of acenaphthaquinone transition metal complexes, Bioinorgan. Chem. Appl. 2021 (2021).
[32] Adem Cinarli, Demet Gurbuz, Tavman Aydin, A. Seher Birteksoz, Synthesis, Characterizations and antimicrobial activity of some Schiff bases of 4-chloro-2-aminophenol, Chem. Soc. Ethiop. 25 (2011).
[33] S.G. Kaplan, L.M. Hanssen, Standard Reference materials.Infrared Transmittance Standard – SRMS 2053,2054,2055 and 2056, NIST Special Publication, 2001.
[34] Hasan Tanak, Aysen Alaman Agar, Orhan Buyukgungor, Experimental (XRD, FT-IR and UV-Vis) and theoretical modelling studies of Schiff base (E)- N1- ((5-nitrothiophen-2-yl)methylene)-2-phenoxyaniline, Spectrochim. Acta Mol. Biomol. Spectrosc. 118 (2014).
[35] Ashraf Sadat Ghasemi, Fereydoun Ashrafi, Javad Sharifi-Rad, Seyedeh Mahsan Hoseini Alfatemi, Molecular structure, spectroscopic assignments and other quantum chemical calculations of anticancer drugs- A review, Cell. Mol. Biol. 61 (2015).
[36] Foziah A. Al-Saif, Spectroscopic, molar conductance and biocidal studies of Pt (IV), Au (III) and Pd (II) chelates of nitrogen and oxygen containing Schiff base derived from 4-Amino antipyrine and 2-Furaldehyde, Int. J. Electrochem. Sci. 61 (2013).
[37] Fatmah A.M.Al-OmaryY. SheenaMaryC. YohannanPanickerAli A.El-EmamIbrahim A.Al-SwaidanAbdulaziz A.Al-SaadiC.Van Alsenoy, Spectroscopic investigations, NBO, HOMO–LUMO, NLO analysis and molecular docking of 5-(adamantan-1-yl)-3-anilinomethyl-2,3-dihydro-1,3,4-oxadiazole-2-thione, a potential bioactive agent, J. Mol. Struct. 1096 (2015).
[38] J. Devi, M. Yadav, D. Kumar, L.S. Naik, D.K. Jindal, Some divalent metal (II) complexes of salicylaldehyde-derived Schiff bases: synthesis, spectroscopic characterization, antimicrobial and invitro anticancer studies, Appl. Organomet. Chem. 33 (2018).
[39] Y.-X. Sun, Q.-L. Hao, W.-X. Wei, Z.-X. Yu, L.-D. Lu, X. Wang, Y.-S. Wang, J. Mol. Struct. (2009).
[40] M. Khaled, M.I.M. Tahir, K.A. Crouse, T. Khoo, Synthesis, characterization , and bioactivity of Schiff bases and their Cd2+, Zn2+, Cu2+ , and Ni2+ complexes derived from chloroacetophenone isomers with S-benzyldithiocarbazate and the X-Ray crystal structure of S-Benzyl- β-N- (4-chlorophenyl)methylened, Bioinorgan 2013 (2013).
[41] A.I. Osman, M. Zolkipli Uwaisulqarni, Daud Fatin Aliyah, Synthesis, characterization and geometry optimization of benzyl 3-[(e,e)-3-phenylprop-2-enylidene]dithiocarbazate (BPED) via DFT studies, J. Sustain. Sci. Manag. 2017 (2017).
[42] Halil Gokce NeomiDege, Onur Erman Dogan, Gokhan Alpaslan, Quantum computational, spectroscopic investigations on N-(2-((2-chloro-4,5-dicyanophenyl) amino)ethyl)-4-methylbenzenesulfonamide by DFT/TD-DFT with different solvents, molecular docking and drug-likeness researches, Coll. Surf. A Physicochem. Eng. Aspect 128311 (2022).
[43] M. Cleiton, L.V. Daniel, L. Modolo, R.B. Alves, M.A. De Resende, C.V.B. Martins, Bases Schiff. A short review of their antimicrobial activities, J. Adv. Res. 2 (2011).
[44] J. Mol. Struct B.D. Joshi, R. Mishra, P. Tandon, A.C. Oliveira, A.P. Ayala, A comparative computational study on molecular structure, NBO analysis, multiple interactions, chemical reactivity and first hyperpolarizability of Imatinib Mesylate polymorphs using DFT and QTAIM approach (GMOS-2013-0048), J. Cheminf. 40 (2014).
[45] K.M. Amin, M.M. Anwar, Y.M. Syam, M.A. Khedr, M.M. Kamel, E.M.A. Kassem, Novel class of substituted spiro [quinazoline-2,1'-cyclohexane] derivatives as effective PPAR-1 inhibitors: molecular modeling, synthesis, cytotoxic and enzyme assay evaluation, Acta Pol. Pharm. 70 (2013).
[46] D.I. Kuntz, A.I. Rosenbaum, F.R. Maxfield, Structure-based strategies for drug design and discovery. Science, Nat. Cent. Biotechnol. Inform. 257 (1992).
[47] J. Drews, Drug discovery: a historical perspective, Science (2000) 1960–1964. Science.org.
[48] Muhammad Imran Abdullah,a, Asif Mahmood,b, Murtaza Madni,c, Sara Masood,d, Muhammad Kashifa, Synthesis, characterization, theoretical, AntiBacterial and molecular docking studies of quinoline based chalcones as A DNA gyrase inhibitor, Bioorg. Chem. 54 (2014).
[49] Asif Mahmood, Muhammad Saqib, Muhammad Ali, Muhammad Imran Abdullah, Bilal Khalid, Theoretical investigation for the designing of novel antioxidants, Can. J. Chem. 91 (2012).
[50] S.F. Sousa, P.A. Fernandes, M.J. Ramos, Protein-ligand docking: current status and future challenges. Proteins, Struct. Funct. Bioinf. 65 (2006).
[51] Muhammad Faizan Nazar, Muhammad Imran Abdullah, Amir Badshah, Asif Mahmood, Usman Ali Rana, Salah Ud-Din Khan, Synthesis, structure–activity relationship and molecular docking of cyclohexenone based analogous as potent non-nucleoside reverse-transcriptase inhibitors, J. Mol. Struct. 1086 (2015).
[52] A.C. Wallace, R.A. Laskowski, Thorutor, A Program to Generate Schematic Diagram of Protein- Ligand Interaction, Protein Eag, 1995.